

Strengthening C–H··· π intermolecular interactions induces emission enhancement of anthracene derivatives under high pressure

Yonghui Lv^a, Xinqi Yang^b, Wenpeng Jia^a, Qian Li^c, Wengang Liu^d, Ben-guo He^e, Yongli Liu^{a,f}, Kai Wang^{c,}, Haichao Liu^{b,*}, Yuxiang Dai^{a,*}*

- a. Department of Materials Physics and Chemistry, School of Materials Science and Engineering, Northeastern University, Shenyang, Liaoning 110819, China.
- b. State Key Laboratory of Supramolecular Structure and Materials, College of Chemistry, Jilin University, Changchun 130012, China.
- c. School of Physics Science and Information Technology, Liaocheng University, Liaocheng, Shandong 252000, China.
- d. School of Resources and Civil Engineering, Northeastern University, Shenyang, Liaoning 110819, China.
- e. Key Laboratory of Ministry of Education on Safe Mining of Deep Metal Mines, Northeastern University, Shenyang, Liaoning 110819, China.

- f. Key Laboratory for Anisotropy and Texture of Materials, Ministry of Education,
Northeastern University, Shenyang, Liaoning 110819, China.

Corresponding Author

Email: daiyuxiang@mail.neu.edu.cn; kaiwang@lcu.edu.cn; hcliu@jlu.edu.cn;

1. Experimental Section

All the reagents and solvents used for synthesis were purchased from commercial source and used without further purification. ^1H and ^{13}C NMR spectra were recorded on Bruker AVANCE 500 and AVANCE III 600 spectrometers, respectively, using tetramethylsilane (TMS) as the internal standard. The mass spectrum was recorded using a Thermo Fisher ITQ1100 instrument. The compounds were characterized by a Flash EA 1112, CHNS elemental analysis instrument. Thermal gravimetric analysis (TGA) was undertaken on a PerkinElmer thermal analysis system at a heating rate of $10\text{ }^\circ\text{C min}^{-1}$ and a nitrogen flow rate of 80 mL min^{-1} . Differential scanning calorimetry (DSC) analysis was carried out using a NETZSCH (DSC-204) instrument at $10\text{ }^\circ\text{C min}^{-1}$ while flushing with nitrogen.

2. Photophysical measurements

Steady-state emission spectra of CZANP in tetrahydrofuran (THF)-water mixed solutions were recorded using an Edinburgh FLS980 Spectrometer. Time-resolved emission spectra of crystals were collected using time-correlated single photon counting (TSCPC) technique on an Edinburgh FLS980 Spectrometer. The photoluminescence quantum yields of crystals under ambient conditions were measured using an Edinburgh FLS980 Spectrometer with its integrate sphere accessory.

3. Single crystal X-ray diffraction (SCXRD) data

Single crystals of CZANP were collected by solvent diffusion method in dichloromethane-methanol system. Single crystals were prepared at room temperature. The diffraction experiments were carried out on a Rigaku R-AXIS RAPID diffractometer equipped with a Mo-K α and control Software using the RAPID AUTO at 293 (\pm 2) °C. The crystal structures were solved with direct methods and refined with a full-matrix least-squares technique using the SHELXS programs.

Crystallographic information:

CZANP, CCDC number: 2393119, a = 8.9902(18) Å, b = 12.532(3) Å, c = 19.733(4) Å, α = 90.00°, β = 90.00°, γ = 90.00°, V = 2223.2(8) Å³, Z = 4, density: 1.253 mg/m³, absorption coefficient: 0.072 mm⁻¹, $F(000)$ = 880, collected reflections: 21652, unique reflections: 5091, R_{int} = 0.0919, Goodness-of-fit on F^2 : 1.000, $R_1 [I > 2\sigma(I)]$ = 0.0549, $\omega R_2 [I > 2\sigma(I)]$ = 0.1080, R_1 (all data) = 0.1074, ωR_2 (all data) = 0.1282.

4. *In situ* high-pressure measurements

All *in situ* high-pressure experiments were implemented using symmetric DAC apparatus furnished with a pair of 400 μ m culet diamonds at room temperature. The CZANP crystals were enclosed into a \sim 150 μ m-diameter hole of the T301 stainless-steel compressible gasket, which was pre-indented to a thickness of 40 μ m. Pressure determination was achieved by the R1 fluorescence spectrum of the ruby.¹ Silicon oil (Aldrich) was utilized

as the pressure transmitting medium (PTM) in the high-pressure PL and UV–vis absorbance experiments. KBr was used as the PTM in IR experiments.

4.1. *In situ* PL and absorption photographs of the samples were obtained using a camera (Canon Eos 5D mark II) equipped on a microscope (Ecclipse TI-U, Nikon). The *in situ* high-pressure UV–vis absorption spectra were measured by a deuterium-halogen light source, and the excitation source. High-pressure PL were measured with an optical fiber spectrometer (Ocean Optics, QE6500) and the 355 nm line of UV DPSS laser was used as the excitation source for PL measurements.

4.2. *In situ* high-pressure IR absorption of CZANP was carried out at room temperature using a Bruker Vertex 70 V FT-IR spectrometer (BRUKER OPTIK GMBH, Germany) in the range of 500–7000 cm^{-1} equipped with a nitrogen-cooled mercury-cadmium-telluride (MCT) detector. The IR major vibrational modes were assigned based on reported studies.²⁻

9

4.3. The X-ray diffraction studies for the CZANP crystal were carried out at the BL15U1 macromolecular crystallography beamline in Shanghai Synchrotron Radiation Facility (SSRF). *In situ* angle dispersive synchrotron X-ray diffraction (ADXRD) experiments with a wavelength of 0.6199 Å were performed at the Advanced Photon Source (APS). CeO_2 was utilized as the standard sample for the calibration. The pattern of intensity versus diffraction angle 2θ was plotted and analysed based on the Dioptas program.¹⁰

4.4. The correction factor (n^2/n_0^2) is reckoned from the Clausius-Mossotti equation and Lorentz-Lorenz equation based on the cell volume under pressure.¹¹⁻¹²

$$\frac{n^2 - 1}{n^2 + 2} \cdot \frac{1}{\rho} = \frac{4\pi}{3} \cdot N_A \cdot \alpha = R_{LL} \#(1)$$

in which the density ρ can be calculated from the cell volume. RLL is called the Lorentz-Lorenz constant. RLL is related to polarizability α . The refractive index n is determined by thin film interference.

4.5. *In situ* high-pressure time-resolved PL measurements of the CZANP crystal in the DAC were measured by home-made setup. A 375 nm pulsed diode laser (LDH-P-C-375B, 40 ps) was used as excitation source. A 20×ultraviolet objective lens was used to project the incident laser onto the sample and collect the backscattered emission signal. The PL signal was directed into the 500 mm focal length grating spectrograph (HRS-500 MS, PI), where a PMT together with a time correlated single photon counting electronics (TimeHarp 260 PICO) was used to detect the PL kinetics.

All decay curves at different pressure were fitted by the double exponential function:

$$I(t) = I_0 + A_1 * \exp(-t/\tau_1) + A_2 * \exp(-t/\tau_2) \#(2)$$

Thus, the average lifetime τ was calculated by the following equation:

$$\tau = \frac{(\mathbf{A}_1 \times \boldsymbol{\tau}_1^2) + (\mathbf{A}_2 \times \boldsymbol{\tau}_2^2)}{(\mathbf{A}_1 \times \boldsymbol{\tau}_1) + (\mathbf{A}_2 \times \boldsymbol{\tau}_2)} \#(3)$$

5. High-pressure geometric optimization

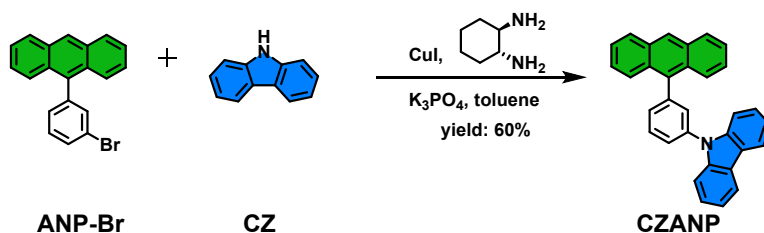
Ab initio calculations of the high-pressure crystal structure were performed by using the pseudopotential plane wave method in the CASTEP package.¹³ The generalized gradient approximation of Perdew-Burke-Ernzerh exchange correlation was used in the geometric optimization with a plane wave cutoff energy of 700 eV.¹⁴

6. Theoretical calculation

Density functional theory (DFT) and time-dependent density functional theory (TD-DFT) calculations were carried out for optimizing the ground state geometry and the lowest excited singlet state (S_1) geometry of CZANP, respectively, at the level of B3LYP/6-31G(d, p) using Gaussian 09 (version D.01) package on a Power Leader cluster. TD-DFT calculations were carried out for the natural transition orbitals (NTOs) at the level of M06-2X/6-31G(d, p).

7. Synthetic details

Synthesis of 9-(3-(anthracen-9-yl)phenyl)-9H-carbazole (CZANP)



9-(3-bromophenyl)anthracene (ANP-Br) was synthesized according to a previously published paper.

A mixture of ANP-Br (199.94 mg, 0.60 mmol), carbazole (167.21 mg, 1.00 mmol), CuI (11.43 mg, 0.06 mmol), (1*R*)-trans-1,2-cyclohexanediamine (40 μ L), K₃PO₄ (1273.60 mg, 6.00 mmol), and 10 mL toluene was degassed and recharged with nitrogen. The mixture was heated by 110 °C and refluxed under a nitrogen atmosphere for 24 h. Then the mixture was extracted with dichloromethane. The organic phase was dried with anhydrous sodium sulfate, filtered and concentrated in vacuum. It was purified via silica gel chromatography by the mixture of petroleum ether/dichloromethane (10:1) to afford the desired compound CZANP in 60% yield (150 mg). ¹H NMR (500 MHz, DMSO-*d*₆, 25 °C, TMS): δ = 8.74 (s, 1H), 8.26 (d, *J* = 7.6 Hz, 2H), 8.20 (d, *J* = 7.8 Hz, 2H), 7.97 (t, *J* = 7.7 Hz, 1H), 7.88 (d, *J* = 8.1 Hz, 1H), 7.76 (d, *J* = 8.1 Hz, 2H), 7.65 – 7.52 (m, 8H), 7.47 (t, *J* = 7.7 Hz, 2H), 7.31 (t, *J* = 7.4 Hz, 2H); ¹³C NMR (151 MHz, CDCl₃, 25 °C, TMS): δ = 140.81 (C), 140.74 (C), 137.95 (C), 135.64 (C), 131.38 (C), 130.22 (CH), 130.18 (C), 129.90 (CH), 129.62 (CH), 128.53 (CH), 128.14 (CH), 127.87 (CH), 127.09 (CH), 126.46 (CH), 126.11 (CH), 126.04 (CH), 125.95 (CH), 125.81 (CH), 125.24 (CH), 123.75 (CH), 123.55 (C), 123.29 (CH),

120.38 (CH), 120.09 (CH), 109.86 (CH).; GC/MS, EI (mass m/z): 419.37 [M⁺]; Anal. calcd

for C₃₂H₂₁N: C 91.62, H 5.05, N 3.34; found: C 92.01, H 5.15, N 3.25.

REFERENCES

- (1) N. H. Chen and I. F. Silvera, *Rev. Sci. Instrum*, 1996, **67**, 4275-4278.
- (2) M. Wu, H. Liu, H. C. Liu, T. Lu, S. P. Wang, G. M. Niu, L. Z. Sui, F. Q. Bai, B. Yang, K. Wang, X. Y. Yang and B. Zou, *J. Phys. Chem. Lett.*, 2022, **13**, 2493-2499.
- (3) P. Hobza and Z. Havlas, *Chem. Rev.*, 2000, **100**, 4253-4264.
- (4) M. Margoshes and V. A. Fassel, *Spectrochimica Acta*, 1955, **7**, 14-24.
- (5) D. H. Whiffen, *J. Chem. Soc.*, 1956, 1350-1356.
- (6) M. Miyazaki and M. Fujii, *Phys. Chem. Chem. Phys*, 2017, **19**, 22759-22776.
- (7) H. S. Yuan, K. Wang, K. Yang, B. B. Liu and B. Zou, *J. Phys. Chem. Lett.*, 2014, **5**, 2968-2973.
- (8) Y. R. Gu, K. Wang, Y. X. Dai, G. J. Xiao, Y. G. Ma, Y. C. Qiao and B. Zou, *J. Phys. Chem. Lett.*, 2017, **8**, 4191-4196.
- (9) H. W. Offen, *J. Chem. Phys.*, 1966, **44**, 699-703.
- (10) C. Prescher and V. B. Prakapenka, *High Pressure Research*, 2015, **35**, 223-230.
- (11) J. Law and R. Rennie, *A Dictionary of Physics*; 6th ed.; Oxford University Press, 2009.
- (12) G. Kleideiter, M. D. Lechner and W. Knoll, *Macromol. Chem. Phys*, 1999, **200**, 1028-1033.
- (13) M. C. Payne, M. P. Teter, D. C. Allan, T. A. Arias and J. D. Joannopoulos, *Rev. Mod. Phys.*, 1992, **64**, 1045-1097.
- (14) J. P. Perdew, K. Burke and M. Ernzerhof, *Phys. Rev. Lett.*, 1996, **77**, 3865-3868.

hole

$S_0 \rightarrow S_1$

particle

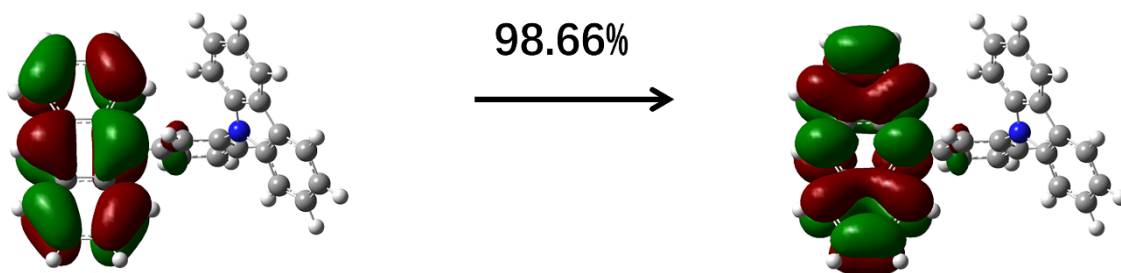


Figure S1. (a) NTO analysis of the CZANP molecule.

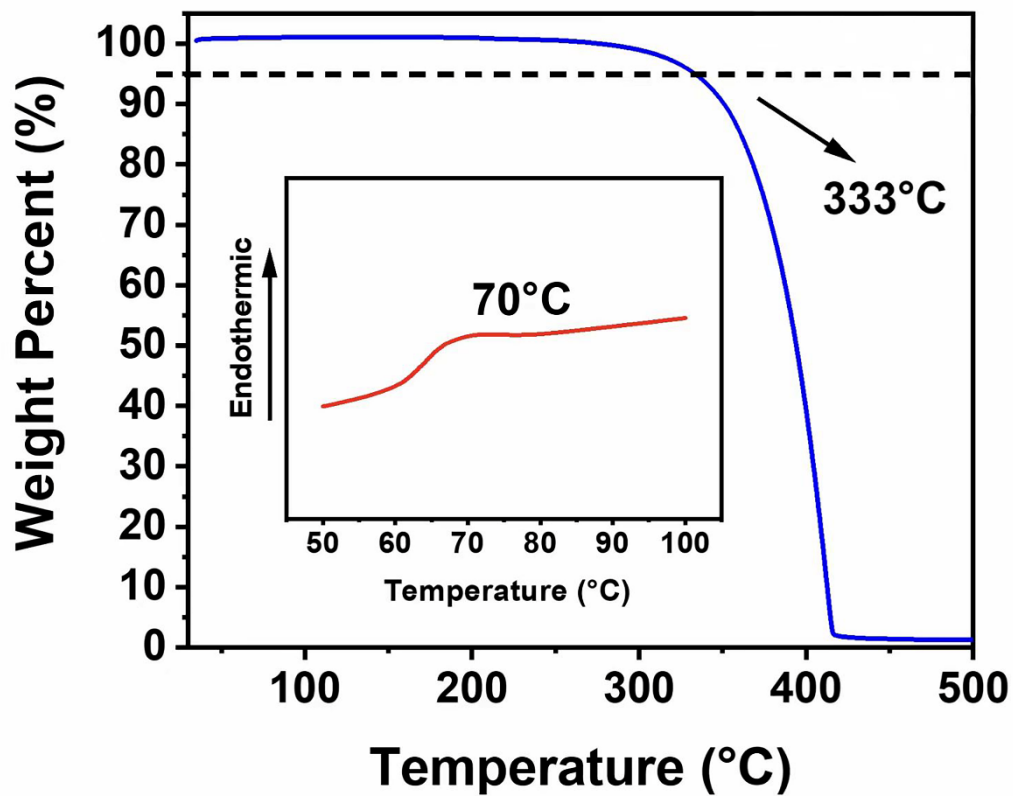


Figure S2. TGA and DSC curves of CZANP crystal.

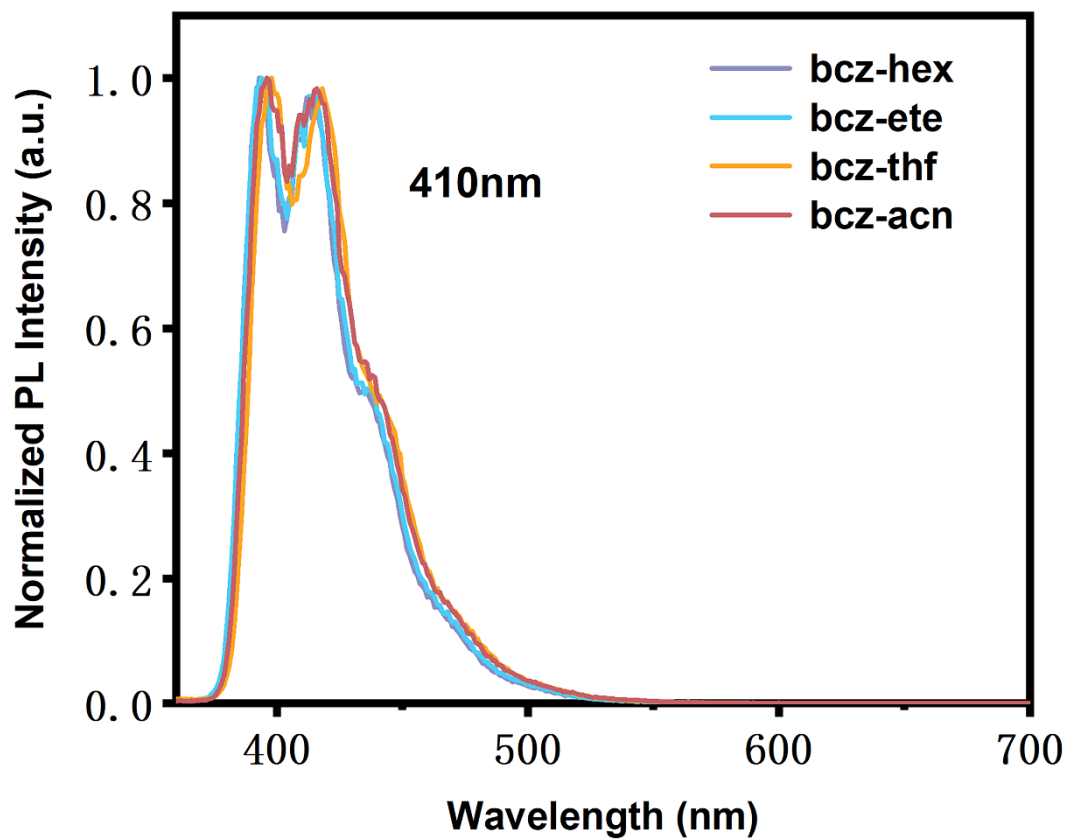


Figure S3. PL spectra of CZANP in different solvents. HEX is hexane, ETE is ethyl ether, THF is tetrahydrofuran, and ACN is acetonitrile.

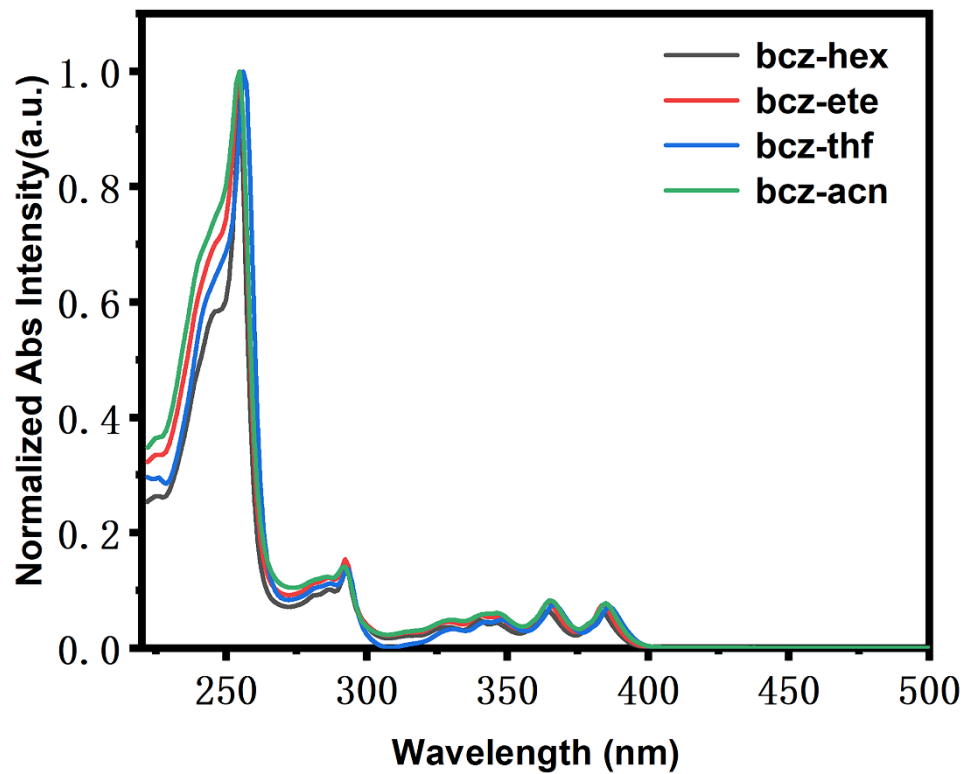


Figure S4. UV-Vis absorption spectra of CZANP in different solvents.

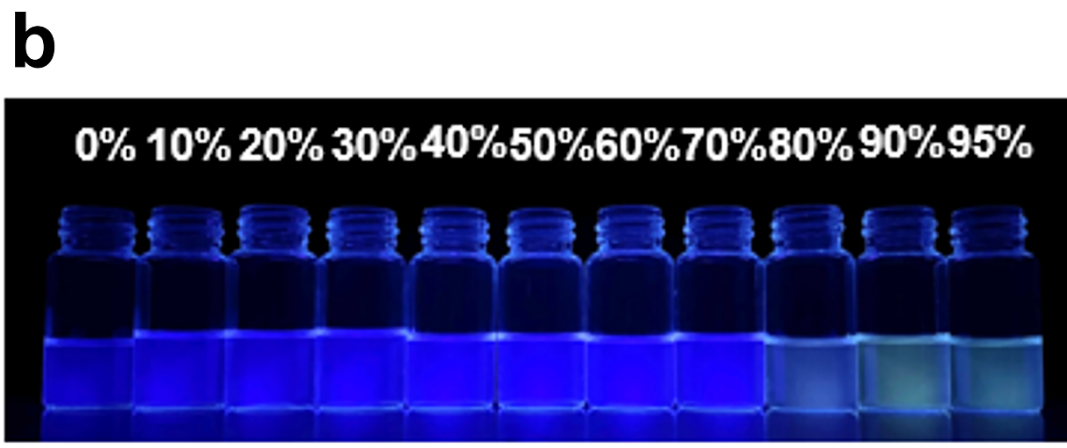
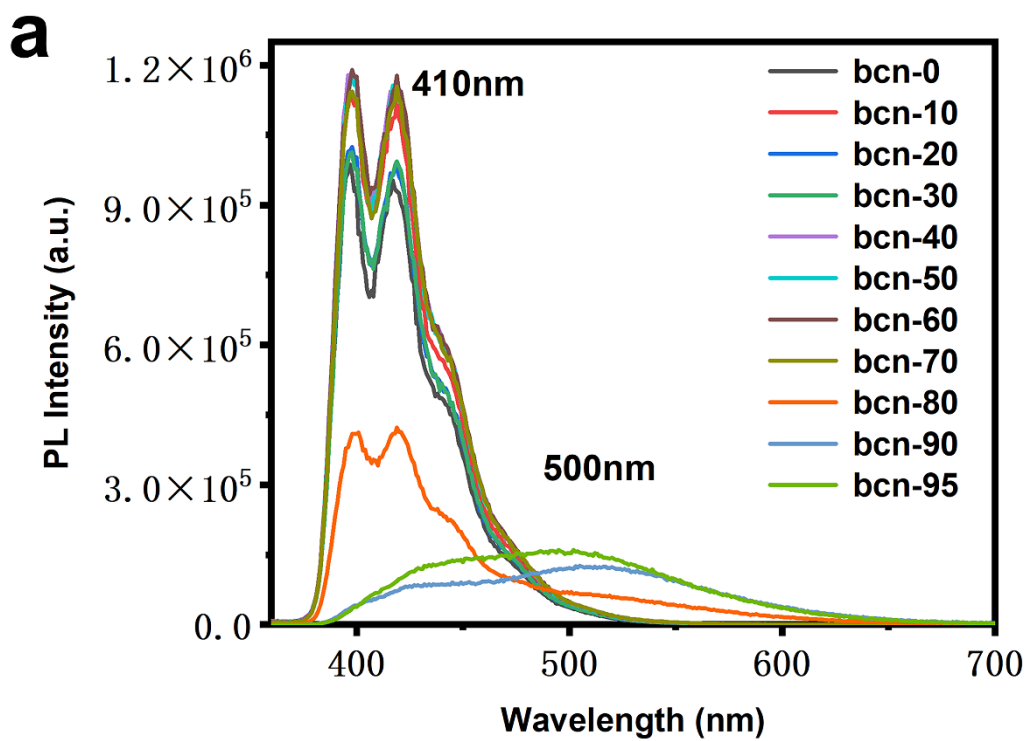


Figure S5. (a) PL spectra of CZANP in mixed water-THF solutions with various water fractions (f_w). (b) Photographs of CZANP in mixed water-THF solutions (the proportions of water are shown on the top) under 365 nm UV lamp irradiation.

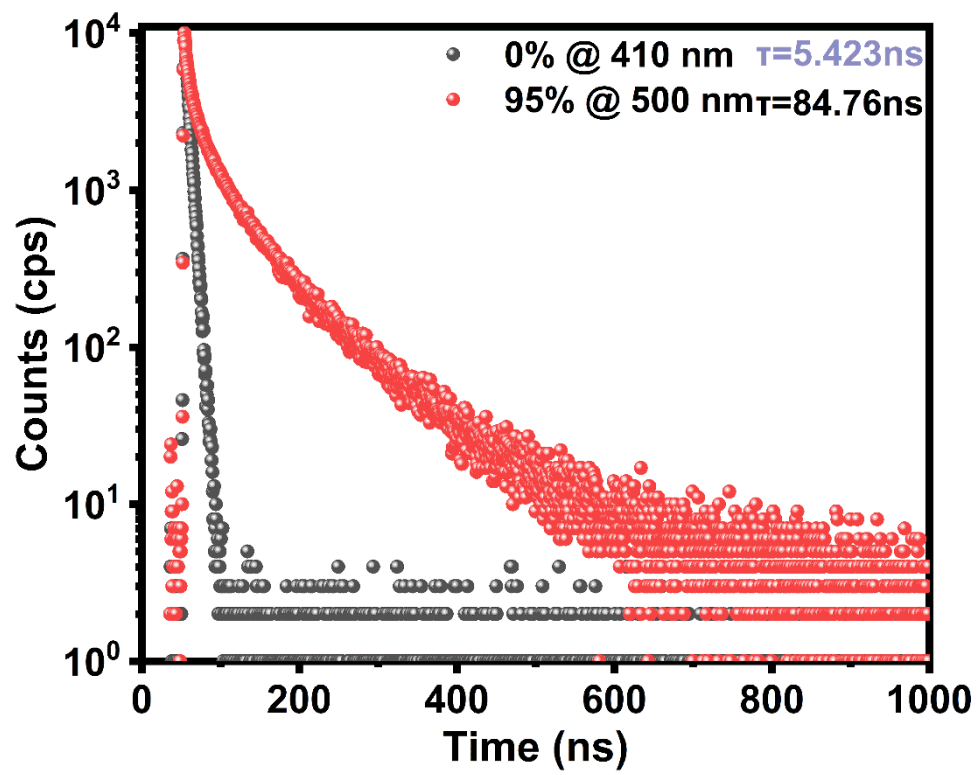


Figure S6. PL decay curves of CZANP in mixed water-THF solutions

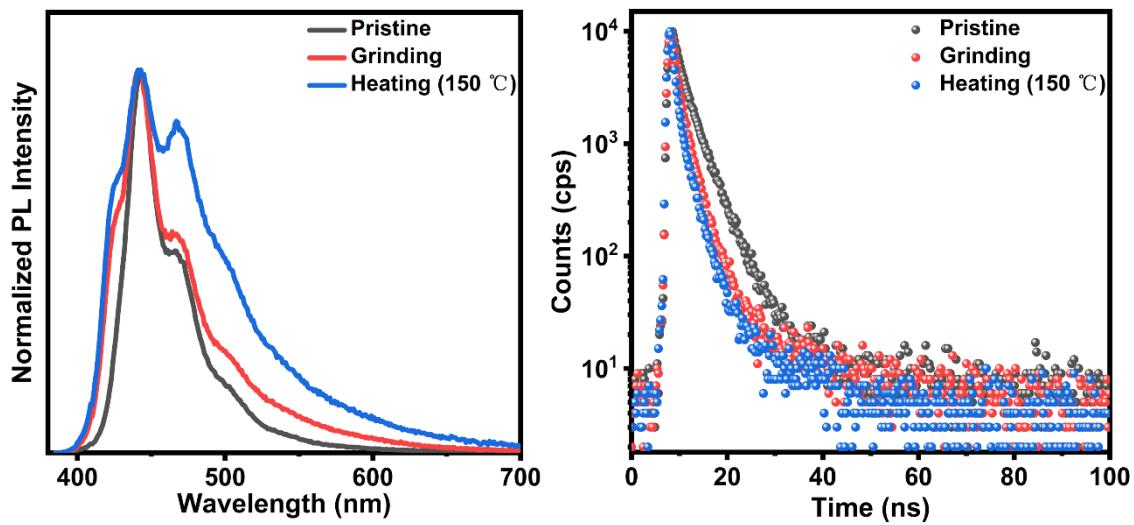


Figure S7. The PL spectra and PL decay curves of ground and heating treated CZANP crystals.

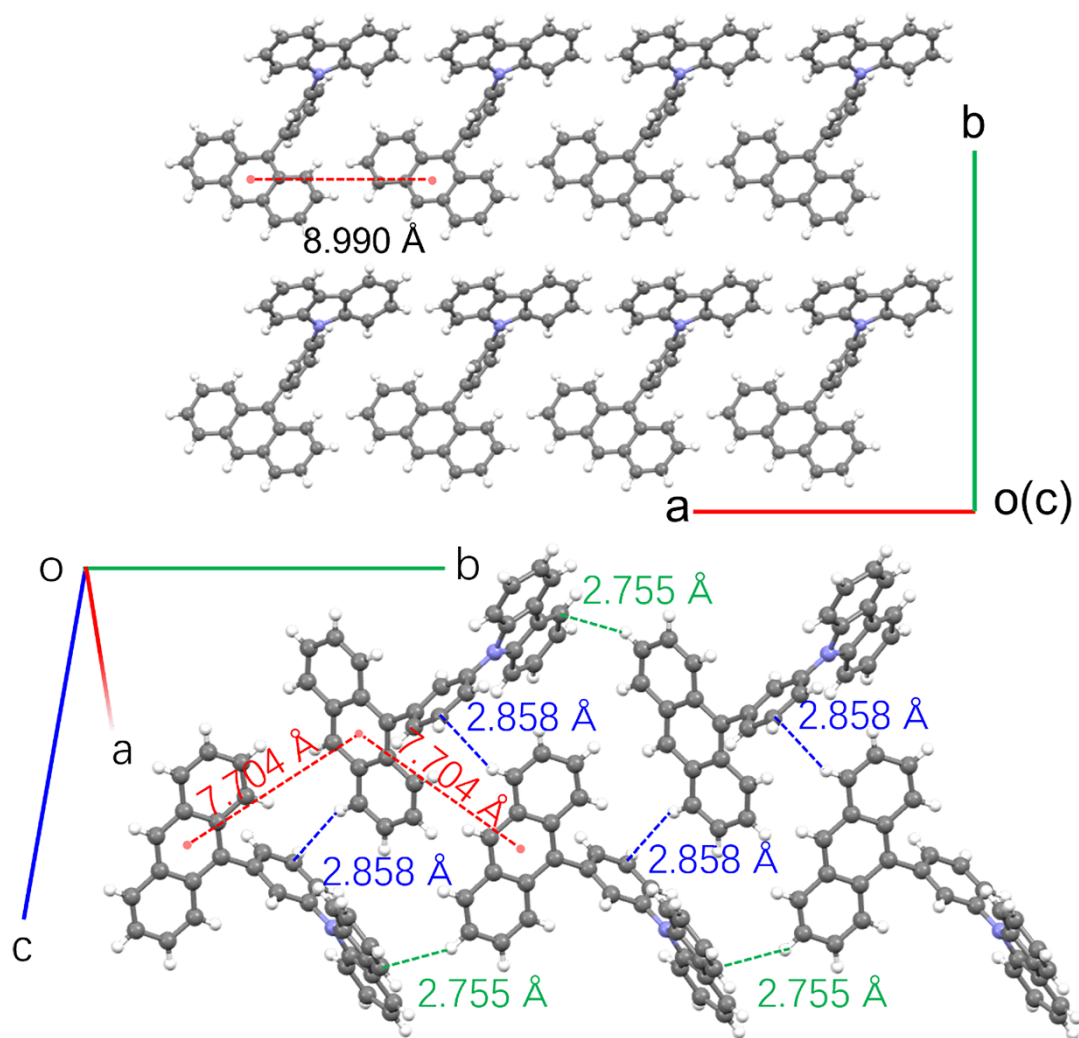


Figure S8. Molecular stacking in the CZANP crystal.

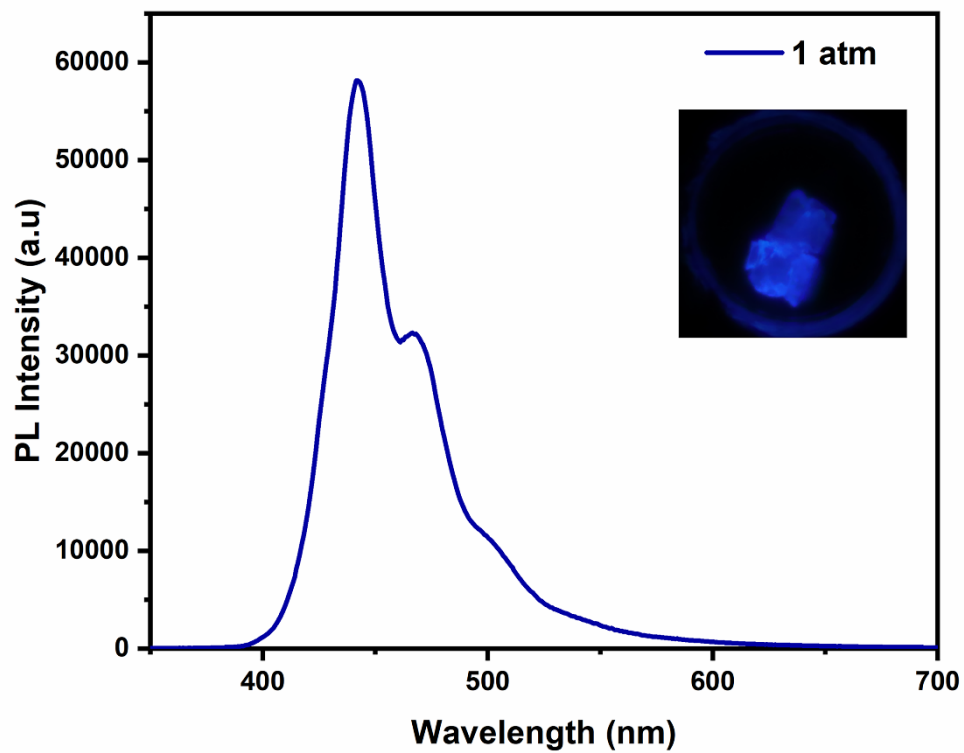


Figure S9. PL spectra of CZANP crystals under ambient conditions excited by a 355nm laser.

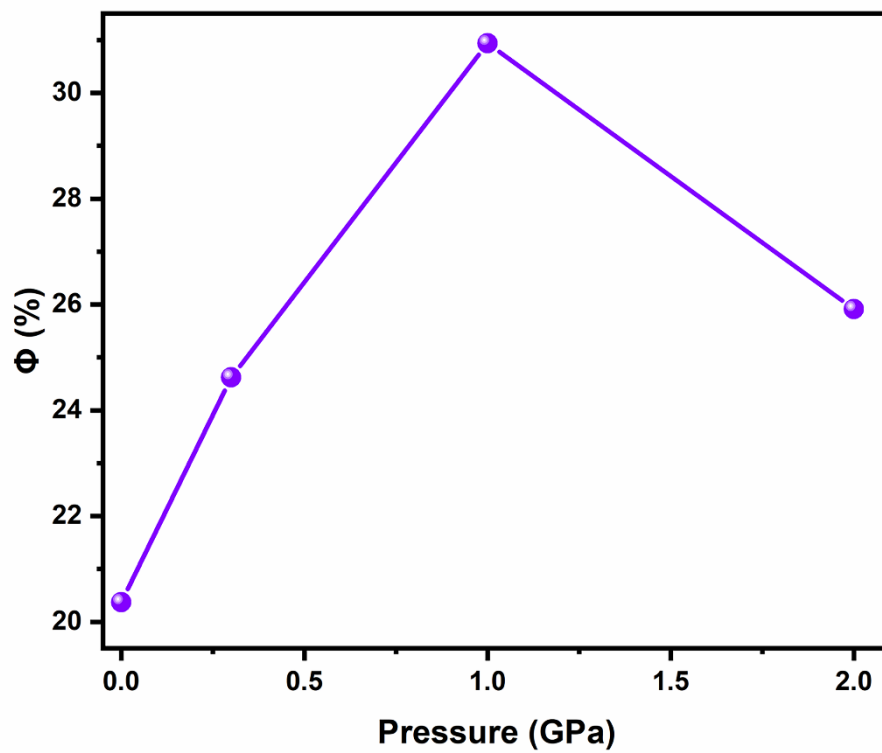


Figure S10. Pressure-dependent Φ evolution of CZANP crystals.

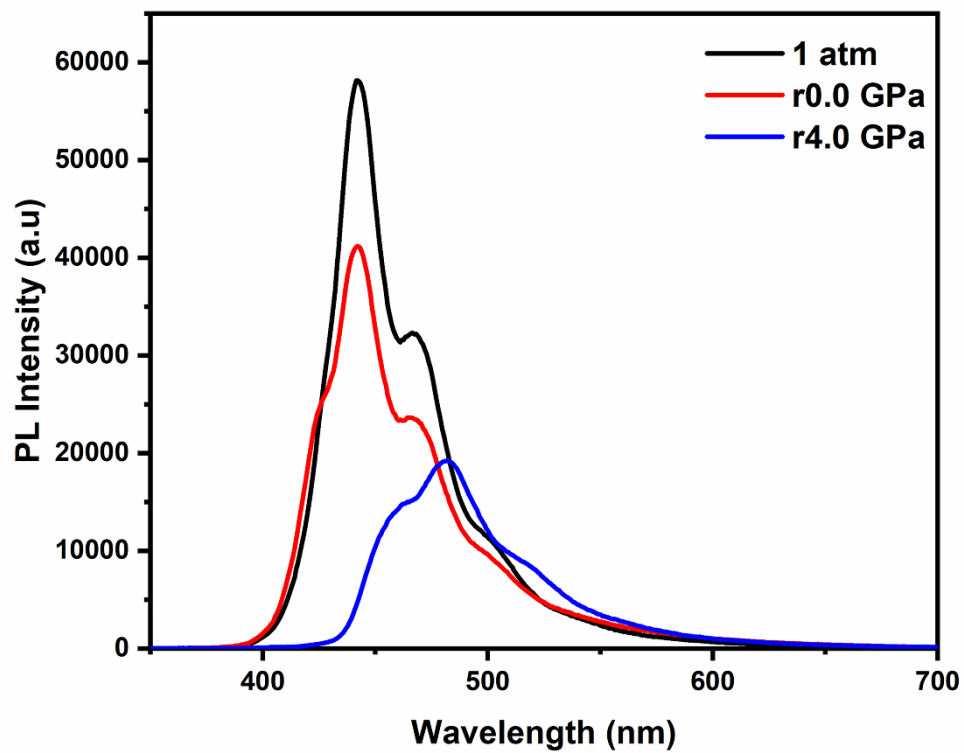


Figure S11. Selected PL spectra excited by a 355 nm laser during decompression of the CZANP crystals (the " r " is the abbreviation of reverse).

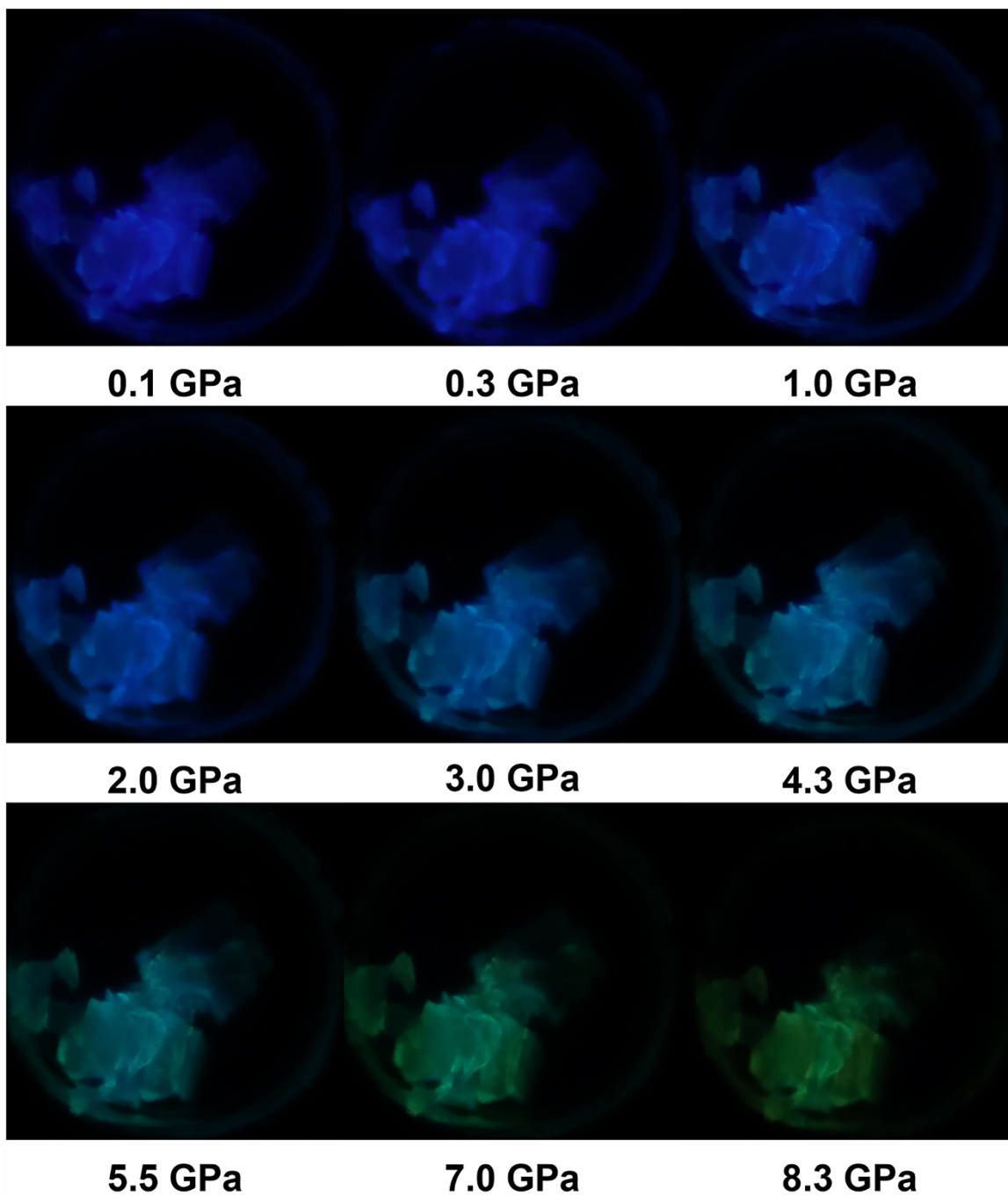


Figure S12. Corresponding fluorescence photographs of the CZANP crystals under the pressure from 1 atm to 8.3 GPa.

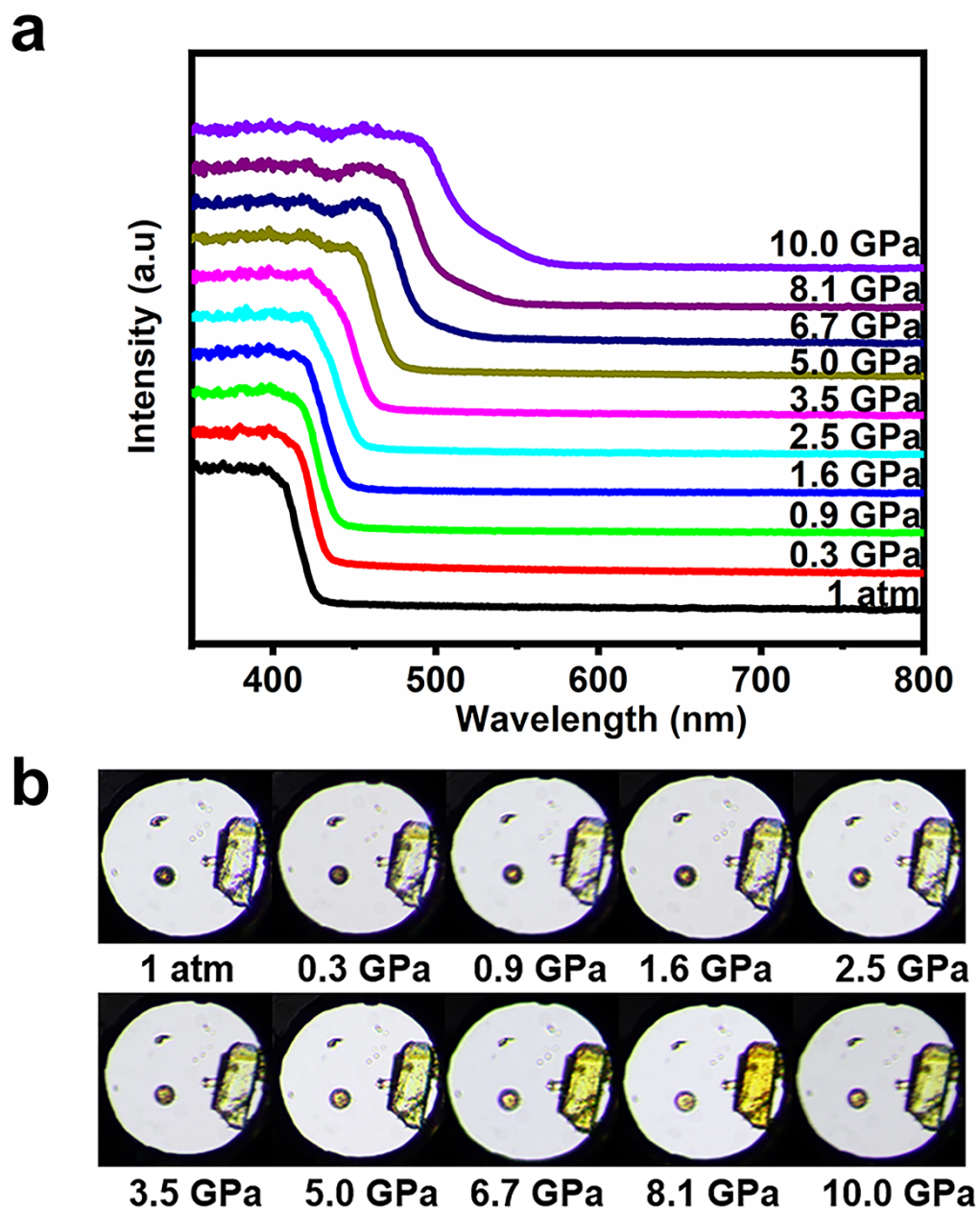


Figure S13. (a) UV–visible absorption spectra of the CZANP crystals at different pressures. (b) Images of normal photographs of the CZANP crystals.

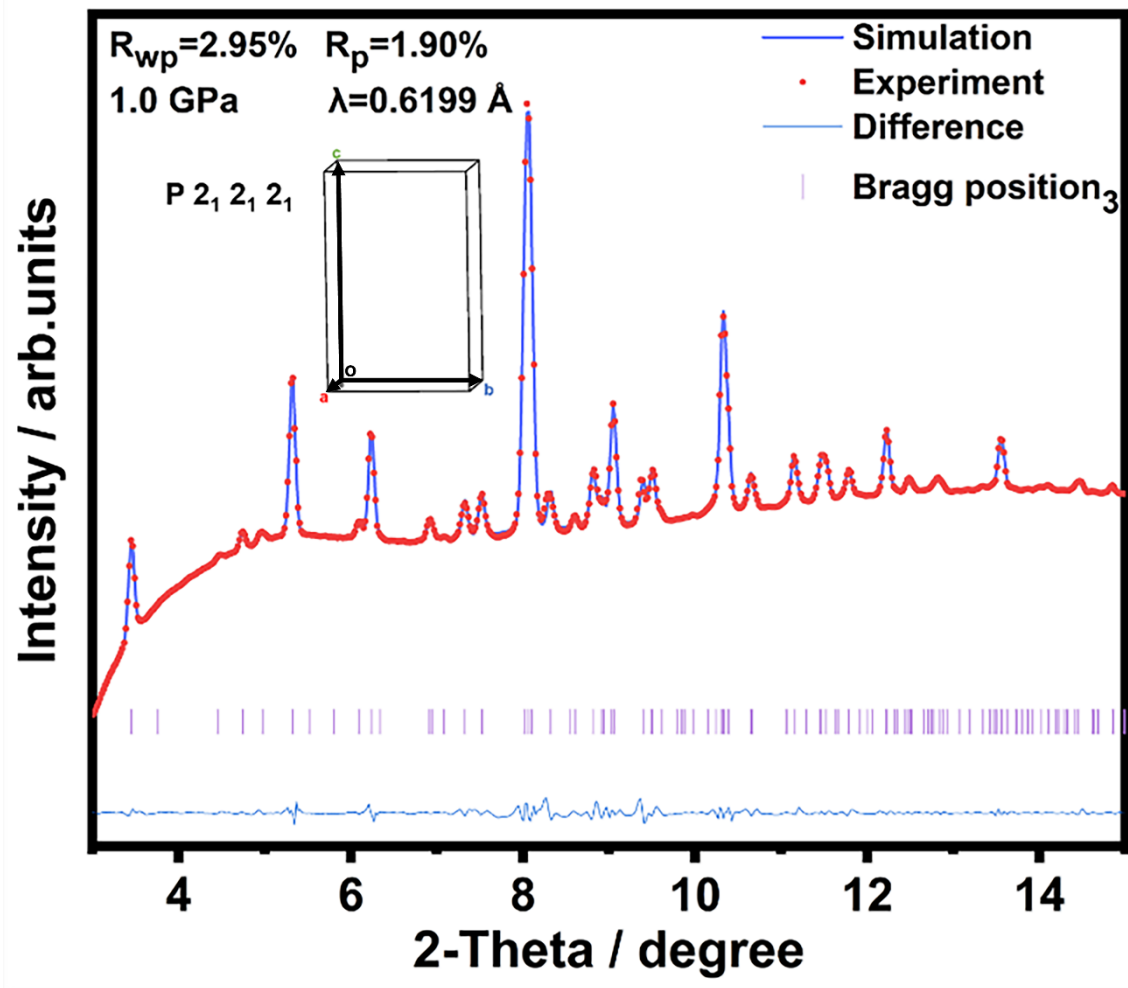


Figure S14. Pawley refinement of the pattern collected at 1.0 GPa

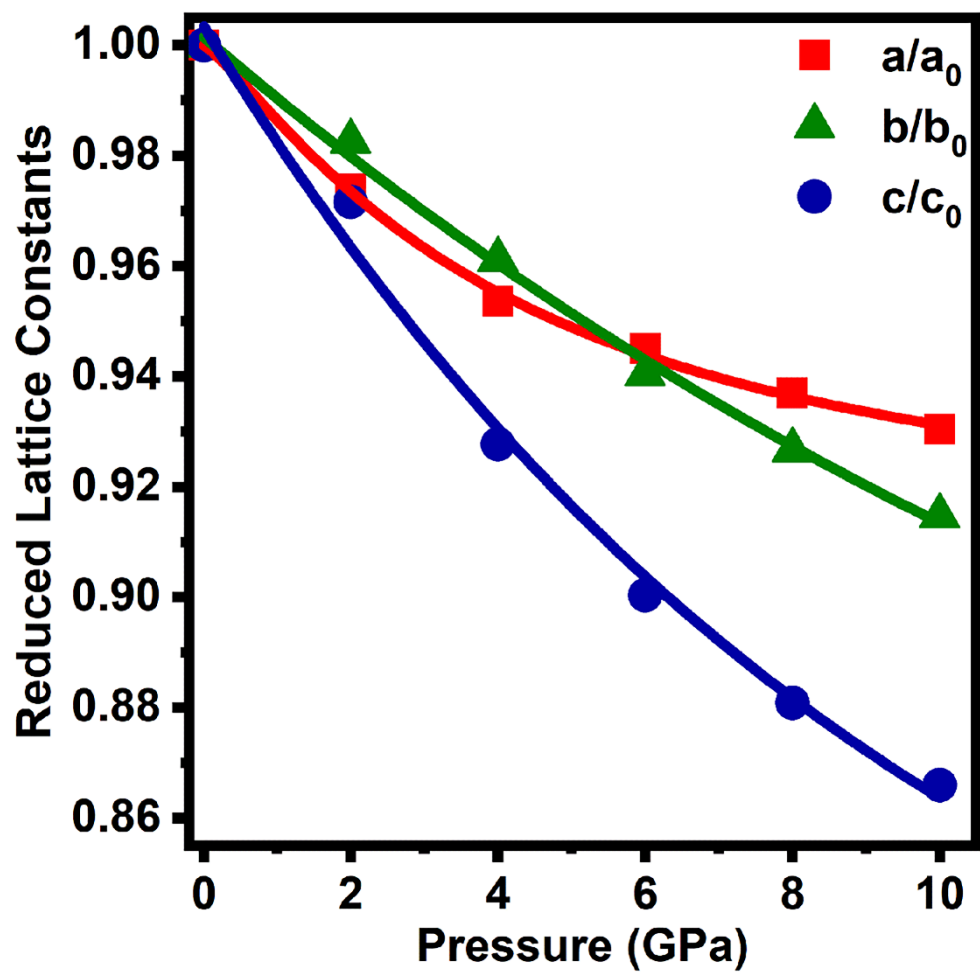


Figure S15. Evolution of the calculated lattice constants.

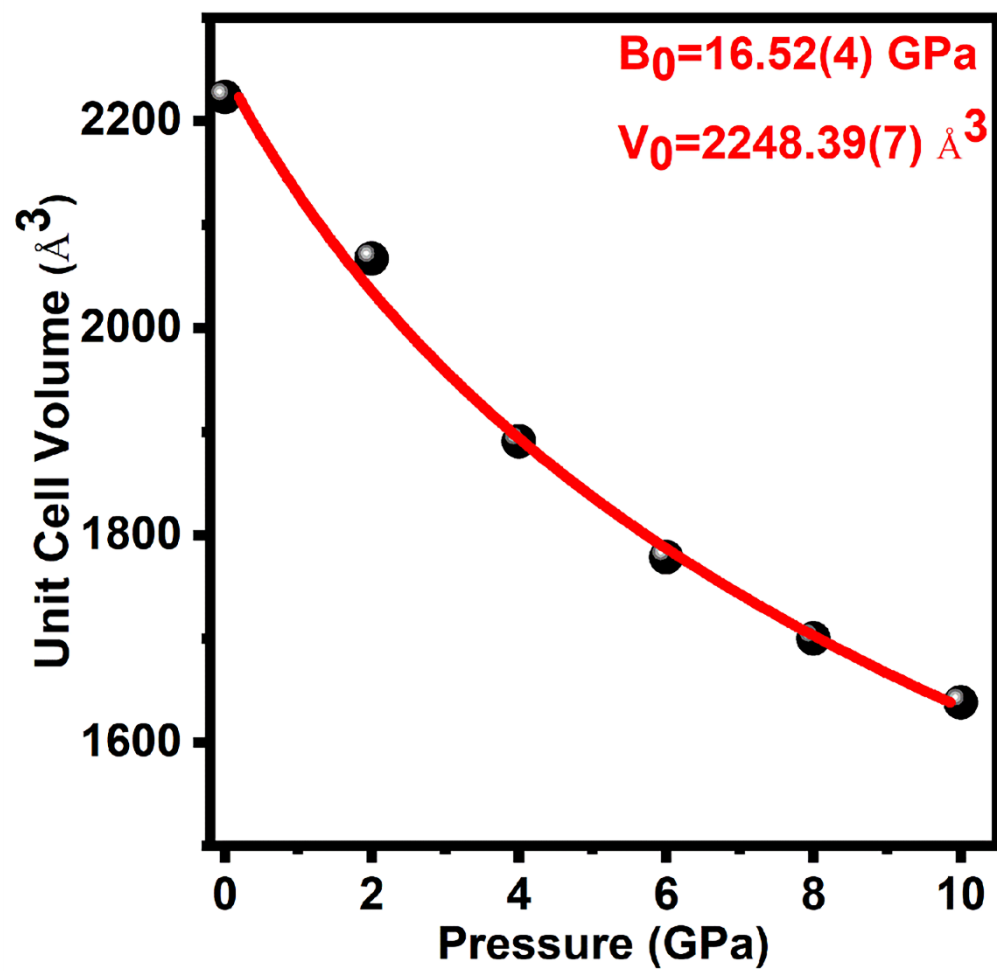


Figure S16. Evolution of the calculated unit cell volume.

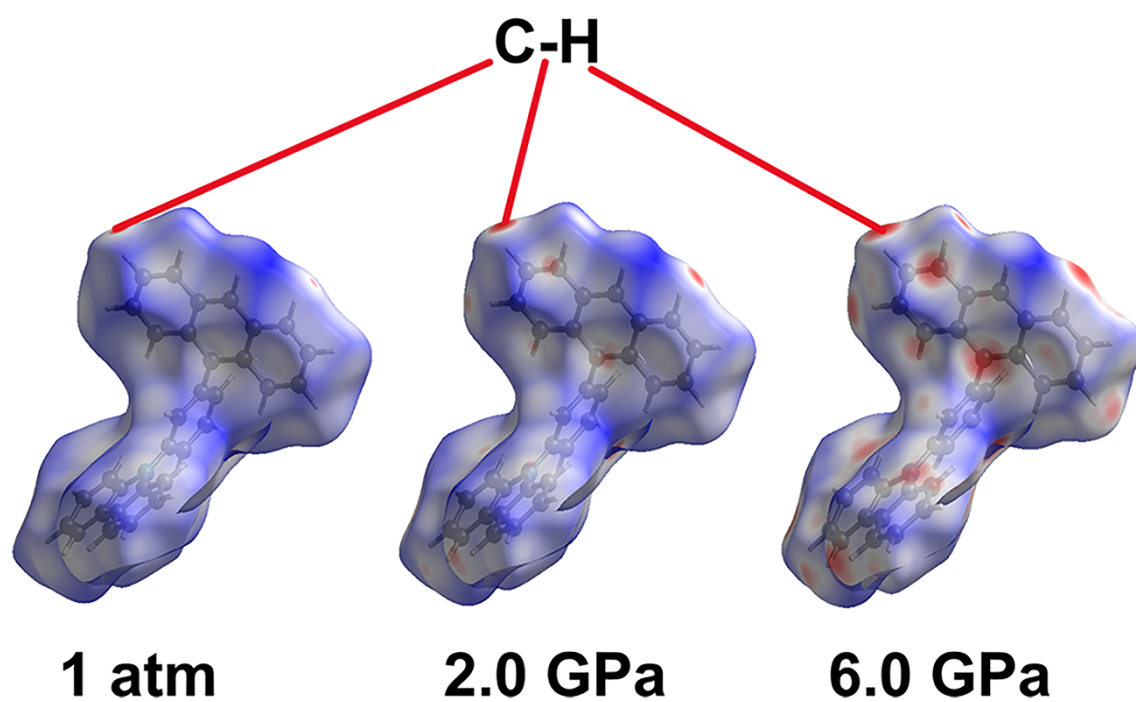


Figure S17. Hirshfeld Surface for the calculated structure at 1 atm, 2.0 GPa, 6.0 GPa mapped with a d_{norm} distance.

Table S1. Pressure dependence of Φ s, average lifetimes and recombination rates of

Pressure (GPa)	PL integral intensity I/I_0	Cell volume V/V_0	Refractive Index square n^2	n^2/n_0^2	Absorbance A_0/A	$\Phi(\%)$
1 atm	1	1	1.96841	1	1	20.37
0.3 GPa	1.0398	0.96047	2.0218	1.027	1.132	24.62
1 GPa	1.1217	0.91297	2.0944	1.064	1.2728	30.94
2 GPa	1.0611	0.89876	2.1182	1.076	1.114	25.91

CZANP crystals.

Pressure (GPa)	τ_1 (ns)	τ_2 (ns)	τ (ns)
0	1.35879	3.97181	3.3
0.3	1.173	4.37812	3.96
1.1	1.83033	5.0512	4.32
2.2	1.58357	4.83276	3.89
3.06	1.40903	5.43836	4.9
4	1.36839	5.7456	5.07
4.97	1.22726	5.55131	4.85
6	1.2887	5.73327	4.93
7.1	1.13534	5.33126	4.59
7.97	1.08223	5.01991	4.27
9.1	1.07312	4.88329	4.02
9.97	0.89097	4.42335	3.61

Table S2. Pressure dependence of lifetime of CZANP crystals.